Validation of results from Barracuda® CFD modelling to predict minimum fluidization velocity and pressure drop of Geldart A particles

Chameera K. Jayarathna[1,2], Britt E. Moldestad[1], Lars-Andre Tokheim[1]

[1]Department of Process, Energy and Environmental Technology, University College of South East Norway, {britt.moldestad, Lars.A.Tokheim}@usn.no

[2]Tel-Tek, Research institute, Porsgrunn, Norway, chameera.jayarathna@tel-tek.no

Abstract

Fluidization characteristics such as the minimum fluidization velocity and the bed pressure drop are important for the design of an efficient fluidized bed. These characteristics can be measured experimentally, but also modelled by CFD simulations. The aim of this study was to use experimental data to validate drag models applied in the CFD software Barracuda.

Most of the drag models available in the literature are validated against Geldart B or D particles and are not necessarily suitable for Geldart A particles, such as the zirconia particles used in the present study. However, by adjusting one of the constants in the Wen-Yu and Ergun drag models, it should be possible to apply these equations also for Geldart A particles.

Data from an in-house built lab-scale fluidized bed unit were used in the study. Reducing the k_1 value in the drag model from 180 to 47 gave a reasonable representation of the minimum fluidization velocity and the pressure drop over the bed.

Keywords: CFD, CPFD, Barracuda, fluidization, pressure drop, minimum fluidization velocity, MP-PIC

1 Introduction

Gas-solids fluidized beds are used in the chemical, energy, and process industries as key equipment units due to their high contact area, homogeneity, heat and mass transfer rates, and solids handling capabilities (Kunii, 1991). Process examples are fluid catalytic cracking (FCC), gasification, combustion of solid fuels, Fischer-Tropsch synthesis, drying, granulation and coating (Cano-Pleite et al., 2017).

The current work is linked to a multistage cross-flow fluidized bed to be applied for high temperature solids classification (Jayarathna et al., 2017). A hot-flow pilot-scale system was downscaled to a cold-flow lab-scale unit by applying Glicksman scaling rules (Glicksman, 1984, 1988, Glicksman et al., 1993).

Computational Fluid Dynamics (CFD) simulations were used as a tool in the design process. Simulations were done for both cold-flow (ambient conditions) and hot-flow systems. The cold-flow experiments were done with a scaled particle mixture, i.e. the particle size and density were not the same as in the hot-flow system (Jayarathna et al., 2017).

The particle mixture contained zirconia particles ($\rho_p = 3800 kgm^{-3}, d_{mean} = 69\mu m$) and steel particles ($\rho_p = 7800 kgm^{-3}, d_{mean} = 290\mu m$). The fluidization behavior of the particles were investigated by Chladek et al. (Chladek et al., 2017) and Amarasinghe et al. (Amarasinghe et al., 2017) applying an in-house built cold-flow cylindrical fluidized bed test unit. The particles were close to spherical (Chladek et al., 2017, Amarasinghe et al., 2017) and could be categorized as Geldart A and D particles, respectively, based on the particle size distribution (PSD), density and the particle fluidization behavior. CFD simulations were also run, using Barracuda® version 17.1, and the simulation results were compared with the experimental observations.

Chladek et al. (Chladek et al., 2017) found that the Barracuda predictions of minimum fluidization velocity was accurate enough for the steel particles, but there was a significant discrepancy for the zirconia particles. Several drag models were used for the simulations and the best results were obtained using the Ergun drag model for steel particles and the Wen-Yu model for zirconia particles.

Amarasinghe et al. (Amarasinghe et al., 2017) did similar CFD simulations and experiments with zirconia, steel and bronze particles, with the aim to evaluate the ability of Barracuda to predict the minimum fluidization velocity of Geldart A (zirconia), B (bronze) and D (steel) particles. The prediction of minimum fluidization velocity (with a combined Wen-Yu/Ergun drag model) was quite good for the Geldart B and D particles, but the simulated results for the Geldart A particles were not in line with the experimental results.

The above-mentioned studies were done with the default drag model settings in Barracuda. In the current study, the results from the minimum fluidization velocity experiments with zirconia particles done by Chladek et al. (Chladek et al., 2017) are used to validate an adjusted

drag model in Barracuda, with the aim to get a better prediction of the fluidization behavior of this Geldart A particle type.

2 CFD Simulations with the MP-PIC method

The CFD simulations applied the multiphase particle-in-cell (MP-PIC) method (Andrews and O'Rourke, 1996, D. M. Snider, 2001), which is also called the computational particle fluid dynamics (CPFD) method (D. M. Snider, 2001). The method is developed based on a new Eulerian–Lagrangian multiphase flow scheme, and the commercially developed platform is known as Barracuda. In this study, version 17.1 was used.

In the MP-PIC method, the real particles in the system are replaced by a computational particle representing a large number of particles which are assumed to behave the same way in the real system. This makes the MP-PIC method more computationally efficient than the more commonly used discrete element method (DEM) (Tsuji et al., 1993, Goldschmidt et al., 2004, Gera et al., 2004), hence it can be applied to larger systems. The CPFD method models the fluid as a continuum and the computational particles as discrete particles exposed to three-dimensional forces as fluid drag, gravity, static–dynamic friction, particle collision and possibly other forces (Dale M. Snider, 2007).

The calculation of particle-to-particle forces in the CPFD method is different from the calculation in the DEM method. In DEM, the particle-to-particle forces are calculated using a spring–damper model and direct particle contact, whereas in the CPFD method collision forces on each particle are modeled as a spatial gradient (Dale M. Snider, 2007). The CPFD method takes into account the forces on a particle hit by other particles, but it does not pay attention to the impact created on the other particles by the first one (Dale M. Snider, 2007). It is common for all other particles as well.

2.1 Model description

The continuity and momentum equations (Gidaspow, 1993) for the gas phase without reactions and interface mass transfer in Barracuda (D. M. Snider, 2001, Gidaspow, 1993) are, given in Equation (1) and (2).

$$\frac{\partial \theta_g \rho_g}{\partial t} + \nabla.\left(\theta_g \rho_g u_g\right) = 0 \tag{1}$$

$$\frac{\partial (\theta_g \rho_g u_g)}{\partial t} + \nabla.\left(\theta_g \rho_g u_g u_g\right) = -\nabla p + \nabla\left(\theta_g \tau_g\right) + \theta_g \rho_g g - F \tag{2}$$

Here $\theta_g, \rho_g, u_g, p, \tau_g$ are the volume fraction (initial), density, velocity, pressure and stress tensor of the gas in the system, respectively. F is the momentum exchange rate per volume between gas and particles, t is the time interval and g is the gravitational acceleration.

The rate of momentum transfer between fluid and solid phases per unit volume (D. M. Snider, 2001, Dale M. Snider et al., 2011) is described in Equation (3).

$$F = \iiint f V_p \rho_p \left[D\left(u_g - u_p\right) - \frac{1}{\rho_p}\nabla p \right] dV_p . d\rho_p . du_p \tag{3}$$

The dynamics of the particle phase are described by the particle probability distribution function $f(x, u_p, \rho_p, V_p, t)$. Here x is the particle position, u_p is the particle velocity, ρ_p is the particle density, V_p is the particle volume, θ_p is the particle volume fraction and D is the drag function. The time evolution of f is obtained by solving a Liouville equation for the particle distribution function (D. M. Snider, 2001), as given in Equation (4).

$$\frac{\partial f}{\partial t} + \nabla\left(f u_p\right) + \nabla u_p . (fA) = 0 \tag{4}$$

The particle acceleration balance A (D. M. Snider, 2001, Andrews and O'Rourke, 1996) is given as,

$$A = D\left(u_g - u_p\right) - \frac{1}{\rho_p}\nabla p + g - \frac{1}{\theta_p \rho_p}\nabla \tau \tag{5}$$

In Barracuda, particle interactions are modelled through the use of a computationally efficient particle stress function. The particle normal stress τ (D. M. Snider, 2001) is a function of particle volume fraction θ_p and is given in Equation (6). The continuum particle stress model used by Snider is an extension of the model from Harris and Crighton (Harris and Crighton, 1994).

$$\tau(\theta_p) = \frac{10 P_s {\theta_p}^{\beta}}{\max\left[\theta_{cp} - \theta_p, \varepsilon\left(1 - \theta_p\right)\right]} \tag{6}$$

Where P_s is a constant with units of pressure, θ_{cp} is the close pack particle volume fraction, β is a constant with a recommended value between 2 and 5, and ε is a very small number. The original expression by Harris and Crighton was modified by Snider to remove the singularity at close pack by adding the ε expression in the denominator. Values for the stress model constant and the close pack volume fraction must be specified by the user.

The default values 1[Pa], 3[-] and 10^{-8}[-] are used for P_s, β and ε respectively.

The fluid drag force on the particles is given in Equation (7). In many models, the drag function (Wen, 1966) is dependent on the fluid conditions, the drag coefficient (C_D), and the Reynolds number (Re). Re is shown in Equation (8).

In many models, the drag function D is related to the to the drag coefficient, as shown in Equation(9).

$$F_p = m_p D(u_g - u_p) \tag{7}$$

$$Re = \frac{2\rho_g r_p |u_g - u_p|}{\mu_g} \quad (8)$$

$$D = \frac{3}{8} C_d \frac{\rho_g |u_g - u_p|}{\rho_p r_p} \quad (9)$$

The Wen-Yu model given in Equation (10) is suitable for dilute systems, and the Ergun model (Ergun, 1952, Beetstra et al., 2007) given in Equation (12) is suitable at higher packing fractions (Gidaspow, 1993). The Wen-Yu/Ergun drag function (Wen, 1966, Patel et al., 1993) combines the Wen-Yu function and the Ergun function, hence can be used for dilute as well as dense systems. The Wen-Yu and Ergun drag function is calculated by Equation (13).

The Wen-Yu model is based on single particle drag models and a dependence on the fluid volume fraction $\theta_g$to account for the particle packing. In the Wen-Yu model, the drag function is calculated by equation (9), and the drag coefficient is a function of the Reynolds number. The model constants are: $c_0 = 1.0, c_1 = 0.15$, $c_2 = 0.44, n_0 = -2.65$ and $n_1 = 0.687$.

$$C_d = \begin{cases} \frac{24}{Re}\theta_g^{n_0} & Re < 0.5 \\ (C_d)_1 & 0.5 \le Re \le 1000 \\ c_2\theta_g^{n_0} & Re > 1000 \end{cases} \quad (10)$$

$$(C_d)_1 = \frac{24}{Re}\theta_g^{n_0}(c_0 + c_1 Re^{n_1}) \quad (11)$$

The Ergun drag model, developed from dense bed data, is given by Equation (12). The model constants are: $k_0 = 2$ and $k_1 = 180$.

$$D = 0.5\left(\frac{k_1\theta_p}{\theta_g Re} + k_0\right)\frac{\rho_g |u_g - u_p|}{\rho_p r_p} \quad (12)$$

Pitault et al. (Pitault et al., 1994) recommended values of 1.75 and 150 for k_0 and k_1, respectively, but in Barracuda the default values are set to 2 and 180.

$$D = \begin{cases} D_1 & \theta_p < 0.75\theta_{CP} \\ D_3 & 0.75\theta_{CP} \ge \theta_p \ge 0.85\theta_{CP} \\ D_2 & \theta_p > 0.85\theta_{CP} \end{cases} \quad (13)$$

$$D_3 = (D_2 - D_1)\left(\frac{\theta_p - 0.75\theta_{CP}}{0.85\theta_{CP} - 0.75\theta_{CP}}\right) \quad (14)$$

Here, D_1 is the Wen-Yu drag function defined in equation (9) and (10), and D_2 is the Ergun drag function defined in equation (12).

3 Computational mesh and input values for the simulation

The cold-flow lab rig-system used to collect data is shown in Figure 1. A three-dimensional cartesian coordinate system was used to describe the vertical cylindrical bed with a diameter of 84 mm and a height of 1.2 m which is 0.3 m shorter than the actual height in order to reduce the computation time. The computational grid is shown in Figure 2 (a). The mesh size was 6.4×6.4×6.4 mm³ and the number of control volumes was around 25 000.

The initial bed height of zirconia solid particles was 17cm. Properties of the zirconia particles are summarized in Table 1.

In the present study, the close pack volume fraction is used as 0.6. Atmospheric air at room temperature was used as the fluidization medium.

The simulation was run for 30 seconds for each air flow rate and increased to the next level. This is also the operational procedure followed in the study of Chladek et al. (Chladek et al., 2017). The total pressure was monitored at positions 2.5 and 12.5 cm above the distributor plate, i.e. at the same positions as in the experiments, as shown in Figure 2 (b). Transient data were recorded for each 0.1 s.

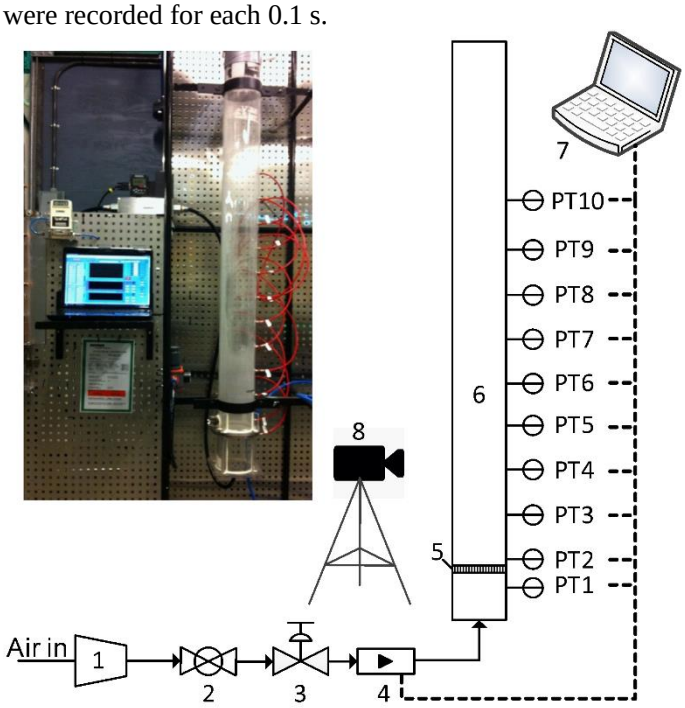

Figure 1: Fluidized bed experimental rig: 1 – compressor, 2 – ball valve, 3 – pressure regulator, 4 – mass flow controller, 5 – air distribution plate, 6 – fluidized bed column, 7 – DAQ and LabVIEW, 8 – video camera.

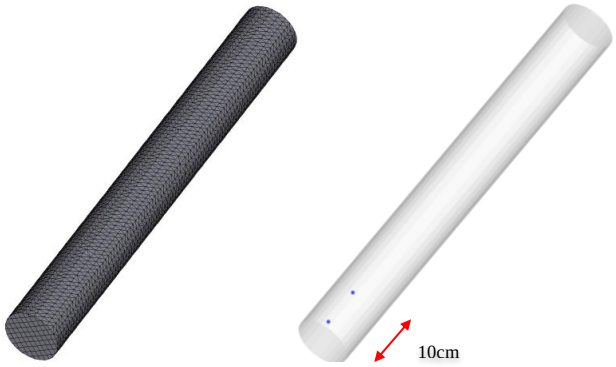

Figure 2: (a) Cylindrical mesh used in the simulations (b) Transient data points for monitoring the total pressure

The properties of the zirconia particles and the steel particles are summarized in Table 1.

Table 1: Properties of the zirconia particles

Property	*Unit*	*Value*
Skeletal density	kg/m3	3830
Bulk density	kg/m3	2270
Particle size range	µm	45-100
D50	µm	70
Porosity	-	0
Sphericity*	-	0.95

* The sphericity was estimated from optical micrographs of the particles.

The combined Wen-Yu/Ergun drag model was used in the present study. The coefficient k_1 was set to different values, and the simulation results were compared with experimental values. The following k_1 values were tried: 180 (default value), 70, 50, 47 and 35.

The average pressure-drop over the particle bed (see Figure 3) in the last 5 seconds of each constant air flow supply period was calculated, assuming that a pseudo steady state was reached after 15 to 25 seconds.

4 Results and discussion

4.1 Adjustment of Wen-Yu/Ergun drag model

As explained above, the combined Wen-Yu/Ergun drag model gives a wide range of accuracy by being able to capture the behavior of both dense and dilute particle systems. Predictions of pressure drop as a function of superficial air velocity at different k_1 values are presented in Figure 3.

According to the Figure 3, the predictions deviate strongly from the measured values when the default k_1 value (180) is used. The reason could be that this model was validated with Geldart B particles, and the original model value (150) is not far from the default value (180) used in Barracuda.

Lowering the coefficient value to 70 or 50 gives more accurate predictions but the predicted stabilized pressure after minimum fluidization velocity are too high. This value is directly connected to the static pressure head of the particle bed or the weight of the particle bed, and it is important that the model can predict this value correctly. A further lowering of coefficient value to 35 gives a too low static pressure head. However, for an intermediate k_1 value of 47, both the pressure and minimum fluidization are predicted quite well. The experimental value and the CFD predictions of the minimum fluidization velocity are then 0.015 and 0.016 m/s, respectively. This shows that correct prediction of the fluidization behavior of Geldart A particles is possible by a drag model adjustment. The potential drawback is that the adjusted model may be valid only for the studied air flow rates. Further studies are needed to investigate a wider range of air flow as the further increased of the airflow will increases the pressure drop and bed will convert from dense to dilute phase.

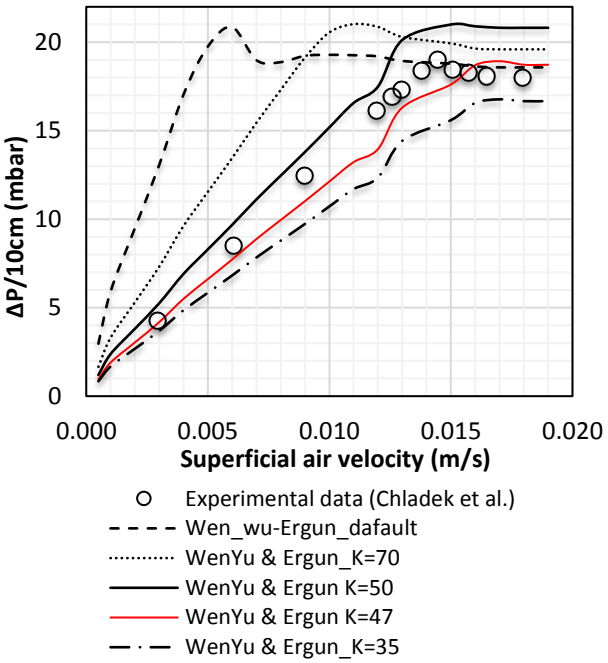

Figure 3: Change of the pressure drop in the bed with increased superficial air flow rate

Lowering the coefficient value to 70 or 50 gives more accurate predictions but the predicted stabilized pressure after minimum fluidization velocity are too high. This value is directly connected to the static pressure head of the particle bed or the weight of the particle bed, and it is important that the model can predict this value correctly. A further lowering of coefficient value to 35 gives a too low static pressure head. However, for an intermediate k_1 value of 47, both the pressure and minimum fluidization are predicted quite well. The experimental value and the CFD predictions of the minimum fluidization velocity are then 0.015 and 0.016 m/s, respectively.

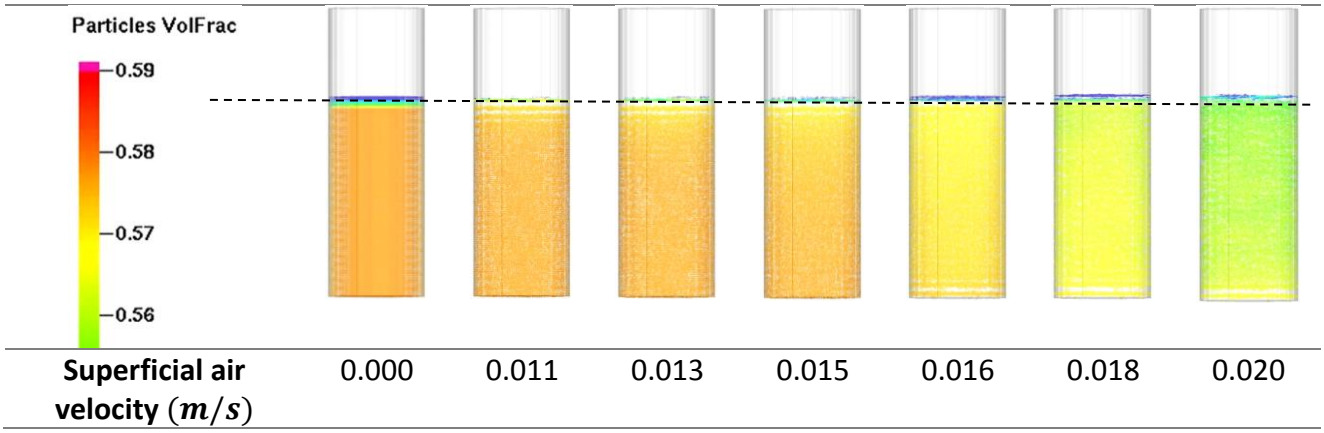

Figure 4: Simulation result snapshots of the lower part of the FB at different superficial air velocities

This shows that correct prediction of the fluidization behavior of Geldart A particles is possible by a drag model adjustment. The potential drawback is that the adjusted model may be valid only for the studied air flow rates. Further studies are needed to investigate a wider range of air flow as the further increased of the airflow will increases the pressure drop and bed will convert from dense to dilute phase.

Figure 4, illustrates the change of solids volume fraction in the bed with the increased air flow rates. At the minimum fluidization velocity (u_{mf}) the weight of the particle bed is balanced by the drag force on the particles and then the gas starts to fluidize the particles. This phenomenon is clearly illustrated in the simulation by the change in color and~ 4%bed expansion with around~4% void fraction increase.

Equation (15) (Rhodes, 2008) explains the connection of the fixed bed pressure drop with the liner coefficient (k_1) of the Ergun drag model. Here x_{sv} is the surface volume diameter (diameter of a sphere having the same volume as the particle).

$$\frac{(-\Delta p)}{H} = \left[k_1 \frac{\mu}{x_{sv}^2} \frac{(1-\theta_g)^2}{\theta_g}\right] |u_g - u_p| + \left[k_0 \frac{\rho_g}{x_{sv}} \frac{(1-\theta_g)}{\theta_g}\right] |u_g - u_p|^2 \quad (15)$$

Equation (15) is only valid for the fixed bed stage before the fluidization but it is clearly indicated liner effect of the coefficient k_1 on the pressure drop as represented in Figure 3 with different k_1 values. As explained by Rhodes (Rhodes, 2008), after the minimum fluidization stage the pressure drop is independent from the relative gas velocity $(u_g - u_p)$. Assuming that in the fluidized bed the entire apparent weight of the particles is supported by the gas flow, then the pressure drop is given by Equation (16) (Rhodes, 2008). According to the equation, the pressure drop is independent of the coefficient k_1.

$$\frac{(-\Delta p)}{H} = (1-\theta_g)(\rho_p - \rho_g)g \quad (16)$$

As explained in the introduction, the role of the drag model is one of the key factors when modelling the fluidization behavior of a dense gas-solids bed, but also other parameters may be important, for example particle-to-wall and particle-to-particle interactions. The model constants related to those phenomena were kept at their default values in this work.

4.2 CFD predictions with BAM

O'Rourke and Snider (O'Rourke and Snider, 2014) developed a new acceleration model called the blended acceleration model (BAM) and it is claimed to give improved predictions of the fluidization behavior of non-uniform (polydisperse) particle collections, i.e. particles of differing sizes or densities. BAM was implemented in Barracuda recently.

A separate simulation was done by using BAM with the Wen-Yu/Ergun drag model (with $k_1 = 47$). Figure 5 shows the results compared with those from applying the Wen-Yu/Ergun drag model (with $k_1 = 47$) without BAM (shown in Figure 4) as well as with the experimental results. The bed pressure-drop predictions at superficial air velocities below the minimum fluidization velocity match the experimental observations when BAM is enabled, but the predictions of the stabilized pressure are higher than the experimental values. However, the simulated minimum fluidization velocity is the same both with and without BAM.

With BAM included, the individual particle accelerations are a blend between the particle acceleration of the original MP-PIC method appropriate for rapid granular flows and an average particle acceleration that applies to closely packed granular flows. As a result, particles at or near close-pack tend to

move together with velocities close to the averaged velocity due to enduring particle-particle contacts. In dilute regions, particles tend to move independently of each other due to less contacts with the surrounding particles (O'Rourke and Snider, 2014). The solids volume fraction of a just fluidized bed is still close to that of the close-pack bed and the particles therefore tend to move together when BAM is enabled.

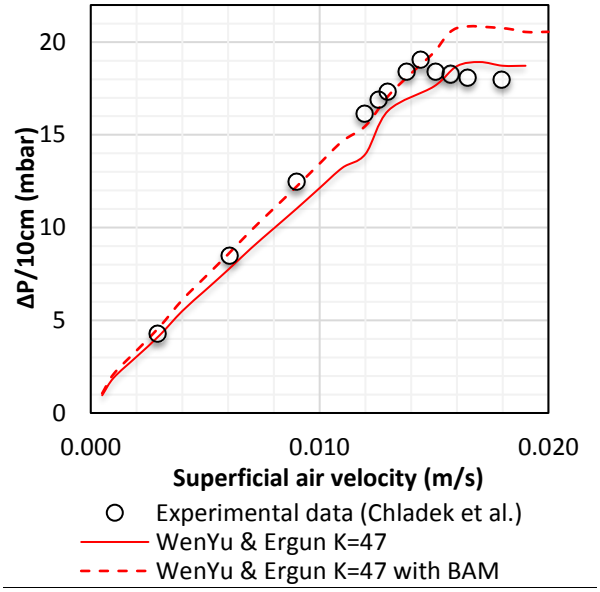

Figure 5: Change of the pressure drop in the bed with increased superficial air flow rate with and without BAM

One of the reasons could be that in the real system, air finds open passages to escape and this leads to a lower stabilized fixed bed pressure drop after the minimum fluidization conditions have been reached. Further investigations of BAM at minimum fluidization conditions of Geldart B and D particles will be useful to come to a better conclusion.

5 Conclusion

By reducing the coefficient k_1 in the Ergun drag model and the combined Wen-Yu/Ergun model from a value of 180 to 47, the CFD predictions of minimum fluidization velocity and pressure drop fit quite well with experimentally measured values for zirconia (Geldart A) particles. For minimum fluidization velocity, the values were 0.015 and 0.016 m/s, respectively. This means that it is possible to give a quite good prediction of the fluidization behavior of Geldart A particles by doing a drag model adjustment.

Barracuda simulations were done with the so-called blended acceleration model (BAM) at $k_1 = 47$. The predications for the fixed bed pressure drop fit well with experimental observations, but the pressure drop after fluidization was somewhat over predicted. One of the reasons could be that in the real system, the air finds open escape passages, and this leads to a lower stabilized fixed bed pressure drop after the minimum fluidization velocity has been reached.

Further investigations of BAM at minimum fluidization conditions for Geldart B and D particles may be useful to come to a better conclusion.

Acknowledgements

The financial support from Gassnova and GE is greatly acknowledged. The authors would also like to thank Sam Clark from CPFD Software, LLC for valuable technical support on Barracuda and Dr. Anette Mathisen from Tel-Tek for commenting on the manuscript.

References

Amarasinghe, W. S., Jayarathna, C. K., Ahangama, B. S., Moldestad, B. M. E. & Tokheim, L.-A. (2017) Experimental study and CFD modelling of fluidization velocity for Geldart A, B and D particles. *International Journal of Modeling and Optimization*, 7, 3.

Andrews, M. J. & O'rourke, P. J. (1996) The multiphase particle-in-cell (MP-PIC) method for dense particulate flows. *International Journal of Multiphase Flow*, 22, 2, p. 379-402.

Beetstra, R., Van Der Hoef, M. A. & Kuipers, J. A. M. (2007) Drag force of intermediate Reynolds number flow past mono- and bidisperse arrays of spheres. *AIChE Journal*, 53, 2, p. 489-501.

Cano-Pleite, E., Hernández-Jiménez, F. & Acosta-Iborra, A. (2017) Bulk oscillation and velocity wave propagation in a vibrated fluidized bed at minimum fluidization conditions. *Powder Technology*, 308, p. 346-361.

Chladek, J., Jayarathna, C. K., Tokheim, L. A. & Moldestad, B. M. E. (2017) Classification of Solid Particles with Size and Density Difference in a Gas Fluidized Bed. *Chemical Engineering Science*, in preparation.

Ergun, S. (1952) Fluid flow through packed columns. *Chemical Engineering Progress*, 48, p. 89.

Gera, D., Syamlal, M. & O'brien, T. J. (2004) Hydrodynamics of particle segregation in fluidized beds. *International Journal of Multiphase Flow*, 30, 4, p. 419-428.

Gidaspow, D. (1993) *Multiphase Flow and Fluidization: Continuum and kinetic theory description.* 24-28 Oval Road, London, Academic Press, Inc.

Glicksman, L. R. (1984) Scaling relationships for fluidized beds. *Chemical Engineering Science*, 39, 9, p. 1373-1379.

Glicksman, L. R. (1988) Scaling relationships for fluidized beds. *Chemical Engineering Science*, 43, 6, p. 1419-1421.

Glicksman, L. R., Hyre, M. & Woloshun, K. (1993) Simplified scaling relationships for fluidized beds. *Powder Technology*, 77, 2, p. 177-199.

Goldschmidt, M. J. V., Beetstra, R. & Kuipers, J. A. M. (2004) Hydrodynamic modelling of dense gas-fluidised beds: comparison and validation of 3D discrete particle and continuum models. *Powder Technology*, 142, 1, p. 23-47.

Harris, S. E. & Crighton, D. G. (1994) Solitons, solitary waves, and voidage disturbances in gas-fluidized beds. *Journal of Fluid Mechanics*, 266, p. 243-276.

Jayarathna, C. K., Chladek, J., Balfe, M., Moldestad, B. M. E. & Tokheim, L. A. (2017) Impact of solids loading and mixture composition on the classification efficiency of a novel cross-flow fluidized bed classifier. *Powder Technology*, In preparation.

Kunii, D. L. O. (1991) *Fluidization engineering.* Boston,Mass., Butterworths.

O'rourke, P. J. & Snider, D. M. (2014) A new blended acceleration model for the particle contact forces induced by an interstitial fluid in dense particle/fluid flows. *Powder Technology*, 256, p. 39-51.
Patel, M. K., Pericleous, K. & Cross, M. (1993) Numerical Modelling of Circulating Fluidized Beds. *International Journal of Computational Fluid Dynamics*, 1, 2, p. 161-176.
Pitault, I., Nevicato, D., Forissier, M. & Bernard, J.-R. (1994) Kinetic model based on a molecular description for catalytic cracking of vacuum gas oil. *Chemical Engineering Science*, 49, 24, p. 4249-4262.
Rhodes, M. J. (2008) *Introduction to particle technology*. Second utg. Chichester ; New York, John Wiley.
Snider, D. M. (2001) An Incompressible Three-Dimensional Multiphase Particle-in-Cell Model for Dense Particle Flows. *Journal of Computational Physics*, 170, 2, p. 523-549.
Snider, D. M. (2007) Three fundamental granular flow experiments and CPFD predictions. *Powder Technology*, 176, 1, p. 36-46.
Snider, D. M., Clark, S. M. & O'rourke, P. J. (2011) Eulerian–Lagrangian method for three-dimensional thermal reacting flow with application to coal gasifiers. *Chemical Engineering Science*, 66, 6, p. 1285-1295.
Tsuji, Y., Kawaguchi, T. & Tanaka, T. (1993) Discrete particle simulation of two-dimensional fluidized bed. *Powder Technology*, 77, 1, p. 79-87.
Wen, C. Y. Y., Y.U. (1966) Mechanics of fluidization. *Chemical Engineering Progress Symposium*, p. 100-111.